

***In situ* photoacoustic analysis of near-infrared absorption of rhodium-doped strontium titanate photocatalyst powder**

Tatsuki Shinoda,^a Yuichi Yamaguchi,^b Akihiko Kudo^b and Naoya Murakami^{*a}

^aGraduate School of Life Science and Systems Engineering, Kyushu Institute of Technology, 2-4 Hibikino, Wakamatsu-ku, Kitakyushu 808-0196, Japan. E-mail: murakami@life.kyutech.ac.jp

^bDepartment of Applied Chemistry, Faculty of Science, Tokyo University of Science, 1-3 Kagurazaka, Shinjuku-ku, Tokyo 162-8601, Japan.

Near-infrared absorption of strontium titanate (SrTiO₃) doped with rhodium (Rh) was investigated by photoacoustic (PA) Fourier transform infrared spectroscopy. In the absence of an electron acceptor and the presence of a hole scavenger, the largest absorption change in the Rh valence state from tetravalent to trivalent was observed in Rh-doped SrTiO₃ prepared at 1473 K, which showed the highest activity for hydrogen evolution. PA measurements revealed the effective redox cycle mechanism between tetravalent and trivalent Rh ions in Rh-doped SrTiO₃.

Photocatalytic water splitting has attracted much attention as an environmentally friendly and low-cost method for direct conversion of solar energy into chemical energy of hydrogen (H_2) gas.^{1,2} Strontium titanate ($SrTiO_3$) has long been known as a photocatalyst for water splitting and it is active for evolution of H_2 and oxygen (O_2) from water during irradiation with ultraviolet (UV) light.³ However, $SrTiO_3$ can absorb only UV light, and visible light-responsivity is required to utilize the inexhaustible supply of solar energy. Hence, metal-ion doping is a useful technique for achieving a response to visible light, and the band gap of wide-gap semiconductors such as $SrTiO_3$ is narrowed by the formation of impurity levels in the forbidden band.² However, the impurity levels often act as recombination centres between photogenerated electrons and holes. It has been reported that $SrTiO_3$ doped with various transition metals (*e.g.*, chromium (Cr), ruthenium (Ru), rhodium (Rh), iridium (Ir) and nickel (Ni)) can respond to light with longer wavelengths and show photocatalytic activities under visible light.^{4–9}

Rh-doped $SrTiO_3$ ($SrTiO_3:Rh$), which possesses a p-type semiconductor character,⁹ can efficiently evolve H_2 gas from an aqueous methanol solution during visible-light irradiation⁵. Accordingly, $SrTiO_3:Rh$ has been used as a H_2 -evolving photocatalyst for artificial Z-scheme systems, and it is a promising material for the achievement of highly efficient H_2 production by water splitting under sunlight.^{2,10,11} In the induction period of a photocatalytic reaction, the Rh valence state changes from tetravalent to trivalent, *i.e.*, trivalent Rh (Rh^{3+}) is produced by the reduction of tetravalent Rh (Rh^{4+}) in the presence of a hole scavenger. Therefore, $SrTiO_3:Rh$ has the unique feature of a change in the valence state of Rh during the reaction, and the role of Rh species in $SrTiO_3:Rh$ is important for the development of photocatalytic activity. Recently, the Rh valence state in $SrTiO_3:Rh$ has been investigated by an electrochemical method,¹² X-ray spectroscopy,¹³ and time-resolved spectroscopy^{14,15}. Previous studies showed that the low activity of $SrTiO_3:Rh^{4+}$ is due to an unoccupied mid-gap state,¹³ and most of photogenerated electrons are trapped at the acceptor levels attributed to Rh^{4+} within 0.14 ps¹⁵. However, there has been no study focusing on the reduction mechanism of Rh^{4+} , *i.e.*, trapping process of electrons into the acceptor levels, during a steady-state photocatalytic reaction.

Photoacoustic spectroscopy (PAS),¹⁶ which is a unique method of detecting photoabsorption as photothermal waves, can be used for *in situ* analysis of the absorption change during a chemical reaction regardless of sample form^{17–20}. In previous studies, we developed a photoacoustic Fourier transform infrared spectroscopy (FTIR-PAS) system for analysing energy levels of trapped electrons in a semiconductor material.^{17,18} A Fourier transform near-infrared (FT-NIR) spectrometer was used for the first time to investigate trap state energetics of semiconductor photocatalyst particles. In the present study, near-infrared (NIR) absorption of $SrTiO_3:Rh$ was observed by using the FTIR-PAS system,

and the dependence of the Rh valence state in SrTiO₃:Rh on preparation temperature and irradiation wavelength was clarified.

SrTiO₃:Rh powders were prepared by a solid-state reaction (SSR) from strontium carbonate (SrCO₃; Kanto Chemical, 99.9%), titanium(IV) oxide (TiO₂; Kojundo Chemical, 99.99%) and rhodium(III) oxide (Rh₂O₃; Wako Chemical, 98-102%) as in a previous study.⁵ The starting materials were mixed at the ratio of Sr:Ti:Rh, corresponding to 1.07:(1-0.01):0.01 for SrTiO₃:Rh(1%) with 7 atom% of excess Sr, and precalcined in air at 1173 K for 1 h. After that, the powders were sintered in air at 1273-1473 K for 5 h or 10 h.

For ultraviolet-visible-near-infrared PAS (UVVISNIR-PAS) measurements, monochromatic light was extracted from a 300 W xenon lamp and halogen lamp using a grating monochromator, and its intensity was modulated by an optical shutter at 12.8 Hz. Measurements were carried out in a closed system at room temperature and 1 atm pressure in the wavelength range of 320-900 nm. The photoacoustic (PA) signal was acquired by a digital MEMS microphone and Fourier-transformed with a Hamming window function. The UVVISNIR-PAS spectra were obtained by normalizing with carbon black powder as a reference.

The FTIR-PAS system has been described in detail in previous reports.^{18,19} The PA cell composed of a duralumin body, a calcium fluoride window, two gas-exchange valves for atmosphere control and a digital MEMS microphone was used. An FT-NIR spectrometer was used as a probe source. Nitrogen (N₂) or O₂ gas containing ethanol vapour was used for controlling the atmosphere in the PA cell. The sample was irradiated with excited light using light-emitting diodes (LEDs) emitting around 365, 455 and 625 nm (Fig. S1), and these intensities were 8.8, 8.4 and 8.4 mW cm⁻², respectively. Measurements were carried out in a closed system at room temperature and 1 atm pressure in the wavenumber range of 15000-2100 cm⁻¹. The PA signal was acquired by a digital MEMS microphone and Fourier-transformed with a Hap-Genzel window function. The FTIR-PAS spectra were obtained by normalizing with carbon black powder as a reference.

In order to observe Rh-related absorption in the visible region, UVVISNIR-PAS measurements were carried out. There was an increase in PA intensity below 390 nm, which is attributed to the band-gap absorption of non-doped SrTiO₃ (Fig. S1a). For SrTiO₃:Rh, broad absorption at around 390-900 nm was seen in addition to UV absorption of SrTiO₃ (Fig. S1b). This absorption was divided into two features: absorption at around 420 nm is attributed to electronic transition from the electron-donor levels formed with Rh³⁺ to the conduction band (CB), while absorption at around 580 nm is ascribed to electronic transition from the valence band (VB) to the electron-acceptor levels formed with Rh⁴⁺ (Fig. 1), indicating that Rh species possess tetravalent and trivalent of the valence state in SrTiO₃:Rh.

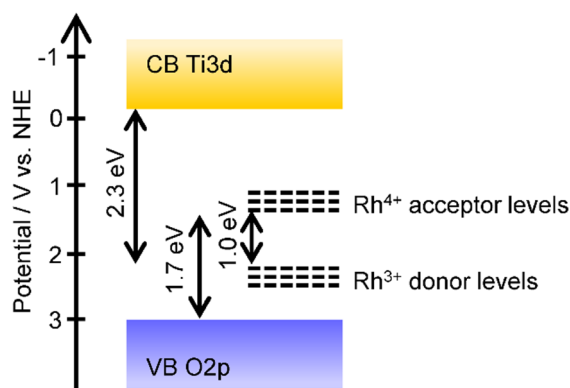


Fig. 1 Proposed energy band diagram of SrTiO₃:Rh.⁵

An FTIR-PAS measurement of SrTiO₃:Rh(1%) was carried out under an N₂ atmosphere in the absence of a hole scavenger. Broad absorption in the range of 15000-5000 cm⁻¹ was observed with Rh doping in comparison with that of non-doped SrTiO₃, and the intensity increased with an increase in the wavenumber (Fig. S2). A broad peak at around 10000 cm⁻¹ and an increase in PA intensity over 11000 cm⁻¹ are attributed to the *d-d* or charge transfer transitions between Rh³⁺ and Rh⁴⁺ species and electronic transition from the VB to the Rh⁴⁺ acceptor levels, respectively (Fig. 1).^{5,9,15} Furthermore, characteristic peaks at around 3400, 5300 and 7300 cm⁻¹ assigned to adsorbed H₂O were observed, while a noise peak at around 3600-4000 cm⁻¹ attributed to H₂O vapour was seen.¹⁸

The same experiment was carried out in the presence of ethanol as a hole scavenger. Fig. 2a shows FTIR-PAS spectra of SrTiO₃:Rh(1%) under an ethanol-saturated N₂ atmosphere. In the dark, Rh⁴⁺ absorption was the same as that under only N₂. Sharp peaks at around 8000-2100 cm⁻¹ were further observed and they are assigned to ethanol. During UV irradiation, PA intensity in the range of 15000-8000 cm⁻¹ decreased with irradiation time. The spectral change in SrTiO₃:Rh(1%) prepared without excess Sr was not seen by UV irradiation as opposed to that in SrTiO₃:Rh(1%) prepared with 7 atom% of excess Sr. (Fig. S3). A control experiment was carried out under an O₂ atmosphere. The spectral shape in the dark was similar to that under an N₂ atmosphere (Fig. 2b). However, unlike that under an N₂ atmosphere, a decrease in PA intensity in the range of 15000-8000 cm⁻¹ was not observed during UV irradiation. Moreover, a change in absorption related to Rh species in the visible region was detected by measuring UVVISNIR-PAS spectra. During UV irradiation, Rh³⁺ absorption increased, whereas Rh⁴⁺ absorption decreased, indicating that the valence state of Rh in SrTiO₃:Rh changed from tetravalent to trivalent (Fig. S4). Consequently, the spectral changes caused by UV irradiation were only seen in the absence of an electron acceptor and the presence of a hole scavenger. These results

suggest that the change in PA intensity is due to the reduction of Rh^{4+} to Rh^{3+} when photoexcited electrons were trapped into the Rh^{4+} acceptor levels.

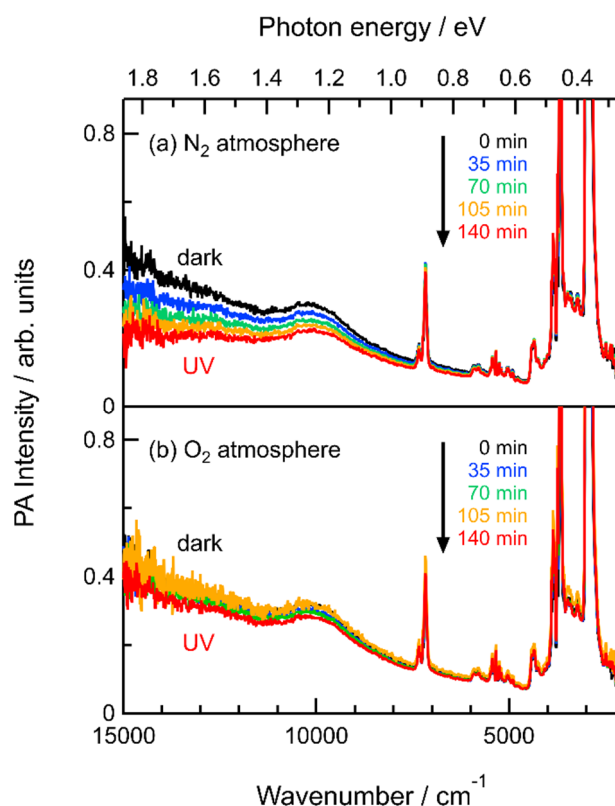


Fig. 2 FTIR-PAS spectra of $\text{SrTiO}_3\text{:Rh(1\%)}$ under ethanol-saturated (a) N_2 and (b) O_2 atmospheres before and during UV irradiation for 140 min. The sample was prepared at 1373 K.

Fig. 3a shows FTIR-PAS spectra of $\text{SrTiO}_3\text{:Rh(1\%)}$ prepared at 1473 K. Rh^{4+} absorption was observed in the dark, while the intensity was higher than that of a sample prepared at 1373 K. The intensity was drastically decreased by UV irradiation, which induced a change in the Rh valence state from tetravalent to trivalent. A sample treated at a low temperature showed different changes (Fig. 3b). Although the spectral shape in the dark was almost the same as that of a sample prepared at 1373 K, during UV irradiation, absorption in the range of $10000\text{--}4000\text{ cm}^{-1}$ increased and absorption in the range of $15000\text{--}10000\text{ cm}^{-1}$ decreased, and this sample had a peak at around 7300 cm^{-1} , corresponding to *ca.* 0.9 eV of photon energy, from a difference spectrum between before and after UV irradiation for 140 min (Fig. S5). The absorption peak resembled that of rutile TiO_2 .¹⁸ For non-doped SrTiO_3 prepared by an SSR at 1373 K, an increase in PA intensity in the range of $12800\text{--}2400\text{ cm}^{-1}$ was observed during UV irradiation, and the peak position was estimated to be 3000 cm^{-1} (0.37 eV) from a difference spectrum between before and after UV irradiation (Fig. S6). A decrease in PA

intensity over 12800 cm^{-1} was seen because of a noise PA signal in the dark, and the change was not due to Rh^{4+} . On the other hand, $\text{SrTiO}_3\text{:Rh}$ samples were prepared with 7 atom% of excess Sr. It has been suggested that an excess amount of Sr suppresses SrO defects, which act as recombination centres of photogenerated electrons and holes.⁷ Actually, time-resolved microwave conductivity measurement revealed that recombination between electrons and holes decreases with an increase in the atomic ratio of Sr/Ti.²¹ Therefore, for $\text{SrTiO}_3\text{:Rh}(1\%)$ prepared at 1273 K, absorption at around $10000\text{--}4000\text{ cm}^{-1}$ is thought to be due to trivalent Ti (Ti^{3+}) species, which generated by accumulation of trapped electrons into Ti sites with oxygen vacancies, as shown in Fig. 3b. The decrease in absorption at around $15000\text{--}10000\text{ cm}^{-1}$ is also attributed to the reduction of Rh^{4+} by trapped electrons; however, there is a possibility that the decrease in absorption during UV irradiation for 35 min was underrated because Ti^{3+} absorption increased and Rh^{4+} absorption decreased at the same time.

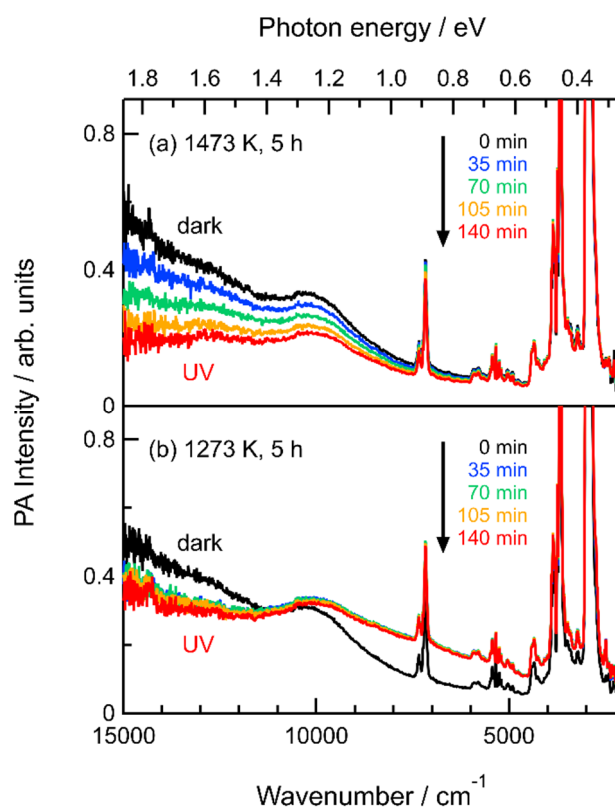


Fig. 3 FTIR-PAS spectra of $\text{SrTiO}_3\text{:Rh}(1\%)$ under an ethanol-saturated N_2 atmosphere before and during UV irradiation for 140 min. Samples were prepared at (a) 1473 and (b) 1273 K.

The Rh^{4+} absorption band at 580 nm possesses the onset of 1.7 eV of photon energy, as reported in the literature (Fig. 1).⁵ Therefore, a decrease in PA intensity of $\text{SrTiO}_3\text{:Rh}$ at 13712 cm^{-1} , corresponding to 1.7 eV of photon energy, was investigated. PA intensity decreased with irradiation time regardless of preparation temperature (Fig. S7). Among the samples, a variation in intensity was clearly observed for the sample treated at a high temperature. This result agrees with photocatalytic activities of $\text{SrTiO}_3\text{:Rh}(1\%)$ (Table S1). Thus, a decrease in PA intensity caused by UV irradiation reflects the amount of reduced Rh^{4+} , indicating that the stability of Rh^{4+} is dependent on preparation temperature.

As explained in the introduction, the Rh valence state changes from tetravalent to trivalent in $\text{SrTiO}_3\text{:Rh}$ in the presence of a hole scavenger. The onsets of absorption, which are due to electronic transitions derived from Rh^{3+} and Rh^{4+} species, have 2.3 and 1.7 eV of photon energy, *i.e.*, *ca.* 540 and 730 nm, respectively (Fig. 1).⁵ Therefore, the dependence of irradiation wavelength was examined by observing spectral changes in $\text{SrTiO}_3\text{:Rh}$ during illumination with excited light. $\text{SrTiO}_3\text{:Rh}(1\%)$ prepared at 1373 K was used as a sample. Fig. S8a shows FTIR-PAS spectra of $\text{SrTiO}_3\text{:Rh}(1\%)$ with adsorbed ethanol under an N_2 atmosphere. In the dark, sharp peaks attributed to ethanol were not clearly observed. The reason for this is that an excess amount of ethanol was removed in order to investigate the change in a steady state under light irradiation for a long time. Strong absorption attributed to Rh^{4+} in comparison with that shown in Fig. 2a was also seen because a sample holder that has less than half the volume of that used in the previous measurement was used, and it is derived from PA signal characteristics that increase with a decrease in the inner volume of the PA cell.¹⁶ During UV irradiation, PA intensity for *ca.* 100 min after starting the illumination was higher than that in the dark. This is probably due to the strong effect of UV-enhanced vibrations of adsorbates on the surface of $\text{SrTiO}_3\text{:Rh}$ particles. After that, a change similar to that with a saturated ethanol condition was observed. The Rh^{4+} absorption recovers to the initial state after exposure to air, and remeasurement showed the same trend (Fig. S9). The sample was photoexcited by irradiation with either blue light or red light or both blue light and red light using LEDs emitting at around 455 or/and 625 nm. Compared to the situation during UV irradiation, blue-light irradiation induced a comparable decrease, whereas the spectral change caused by red-light irradiation was small (Fig. S10). However, Rh^{4+} absorption was drastically decreased by simultaneous irradiation with blue light and red light (blue + red light) in comparison with that during UV irradiation (Fig. S8b). Therefore, the degree of decrease in PA intensity was large in the order of blue + red > UV \approx blue > red light irradiation (Fig. 4), indicating that the difference in spectral changes depends on irradiation wavelength. In the case of irradiation with UV light or blue light, Rh^{4+} is reduced by trapping of photoexcited electrons in the CB (Fig. S11a and b), while Rh^{4+} is reduced by electronic transition from the VB to the Rh^{4+} acceptor

levels during red-light irradiation (Fig. S11c). Thus, simultaneous irradiation with blue + red light induces the reduction of Rh^{4+} by two kinds of electronic transition: one is from the Rh^{3+} donor levels to the CB and the other is from the VB to the Rh^{4+} acceptor levels (Fig. S11d). The number of photons affects the decrease in PA intensity under excited light irradiation, especially in the same case of electron-transfer mechanism.

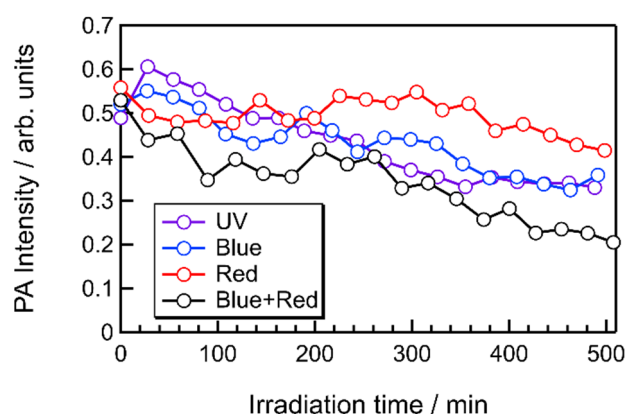


Fig. 4 Decrease in PA intensity of $\text{SrTiO}_3\text{:Rh}(1\%)$ at 13712 cm^{-1} during excited light irradiation. Measurements were carried out in the presence of surface-adsorbed ethanol under an N_2 atmosphere. The sample was irradiated with excited light using LEDs emitting around 365, 455 and 625 nm.

In conclusion, NIR absorption attributed to the impurity levels formed with Rh species in $\text{SrTiO}_3\text{:Rh}$ was measured by FTIR-PAS using an FT-NIR spectrometer. In the absence of an electron acceptor and the presence of a hole scavenger, there was a decrease in Rh^{4+} absorption with excited light irradiation, which is ascribed to the reduction of Rh^{4+} to Rh^{3+} , suggesting that the spectral change depends on preparation temperature and reflects the amount of reduced Rh^{4+} . On the other hand, measurement during simultaneous irradiation with blue + red light showed a large change in comparison with that under other excitation-wavelength conditions. Therefore, the results indicate that a highly effective redox cycle between Rh^{4+} and Rh^{3+} is important for photocatalytic reactions using $\text{SrTiO}_3\text{:Rh}$. Thus, FTIR-PAS is a powerful tool for measurement of impurity levels formed by metal-ion doping in semiconductor materials.

This work was supported by a Grant-in-Aid for Scientific Research(C) (Grant number 17K06019), a Grant-in-Aid for Scientific Research on Innovative Areas “Innovations for Light-Energy Conversion (I^4LEC)” (Grant number 18H05172) and a Grant-in-Aid for JSPS Fellows (Grant number 20J23117). The authors thank Mr. Kenta Watanabe and Mr. Yuhei Udagawa for sample preparation.

Conflicts of interest

There are no conflicts to declare.

Notes and references

- 1 A. Kudo and Y. Miseki, *Chem. Soc. Rev.*, 2009, **38**, 253–278.
- 2 K. Domen, S. Naito, M. Soma, T. Onishi and K. Tamaru, *J. Chem. Soc., Chem. Commun.*, 1980, 543–544.
- 3 H. Kato and A. Kudo, *J. Phys. Chem. B*, 2002, **106**, 5029–5034.
- 4 R. Konta, T. Ishii, H. Kato and A. Kudo, *J. Phys. Chem. B*, 2004, **108**, 8992–8995.
- 5 R. Niishiro, S. Tanaka and A. Kudo, *Appl. Catal., B*, 2014, **150–151**, 187–196.
- 6 H. Kato, Y. Sasaki, N. Shirakura and A. Kudo, *J. Mater. Chem. A*, 2013, **1**, 12327–12333.
- 7 R. Niishiro, H. Kato and A. Kudo, *Phys. Chem. Chem. Phys.*, 2005, **7**, 2241–2245.
- 8 K. Iwashina and A. Kudo, *J. Am. Chem. Soc.*, 2011, **133**, 13272–13275.
- 9 Y. Sasaki, H. Nemoto, K. Saito and A. Kudo, *J. Phys. Chem. C*, 2009, **113**, 17536–17542.
- 10 A. Kudo, S. Yoshino, T. Tsuchiya, Y. Udagawa, Y. Takahashi, M. Yamaguchi, I. Ogasawara, H. Matsumoto and A. Iwase, *Faraday Discuss.*, 2019, **215**, 313–328.
- 11 S. Kawasaki, K. Nakatsuji, J. Yoshinobu, F. Komori, R. Takahashi, M. Lippmaa, K. Mase and A. Kudo, *Appl. Phys. Lett.*, 2012, **101**, 003910.
- 12 S. Kawasaki, K. Akagi, K. Nakatsuji, S. Yamamoto, I. Matsuda, Y. Harada, J. Yoshinobu, F. Komori, R. Takahashi, M. Lippmaa, C. Sakai, H. Niwa, M. Oshima, K. Iwashina and A. Kudo, *J. Phys. Chem. C*, 2012, **116**, 24445–24448.
- 13 K. Furuhashi, Q. Jia, A. Kudo and H. Onishi, *J. Phys. Chem. C*, 2013, **117**, 19101–19106.
- 14 D. H. K. Murthy, H. Matsuzaki, Q. Wang, Y. Suzuki, K. Seki, T. Hisatomi, T. Yamada, A. Kudo, K. Domen and A. Furube, *Sustainable Energy Fuels*, 2019, **3**, 208–218.
- 15 A. Rosencwaig and A. Gersho, *J. Appl. Phys.*, 1976, **47**, 64–69.

- 16 N. Murakami and T. Shinoda, *Phys. Chem. Chem. Phys.*, 2018, **20**, 24519–24522.
- 17 T. Shinoda and N. Murakami, *J. Phys. Chem. C*, 2019, **123**, 12169–12175.
- 18 N. Murakami and N. Koga, *Catal. Commun.*, 2016, **83**, 1–4.
- 19 N. Murakami and T. Shinoda, *J. Phys. Chem. C*, 2019, **123**, 222–226.
- 20 K. Yamada, H. Suzuki, R. Abe and A. Saeki, *J. Phys. Chem. Lett.*, 2019, **10**, 1986–1991.